

GENUS STATISTICS OF THE LARGE-SCALE STRUCTURE WITH NON-GAUSSIAN DENSITY FIELDS

TAKAHIKO MATSUBARA

Department of Physics, University of Tokyo, Tokyo 113, Japan

AND

JUN'ICHI YOKOYAMA¹

Uji Research Center, Yukawa Institute for Theoretical Physics, Kyoto University, Uji 611, Japan

Received 1995 September 12; accepted 1995 December 13

ABSTRACT

As a statistical measure to quantify the topological structure of the large-scale structure in the universe, the genus number is calculated for a number of non-Gaussian distributions in which the density field is characterized by a nontrivial function of some Gaussian-distributed random numbers. As a specific example, the formulae for the lognormal and χ^2 distributions are derived and compared with the results of *N*-body simulations together with the previously known formulae for the Gaussian distribution and second-order perturbation theory. It is shown that the lognormal formula fits most of the simulation data the best.

Subject headings: cosmology: theory — large-scale structure of universe — methods: numerical — methods: statistical

1. INTRODUCTION

One of the most important purposes of observational cosmology is to extract the power spectrum and the statistical distribution of primordial fluctuations out of the redshift survey of large-scale structure, in order to single out the correct model of the evolution of our universe. A number of measures have been used to characterize statistical properties of the large-scale structure. The most commonly used quantity is the two-point correlation function (Totsuji & Kihara 1969), which is nothing but the Fourier transform of the power spectrum and so does not contain much information on the large-scale structure's statistical distribution. On the other hand, the count-in-cells statistic including the void probability (White 1979), directly measures the statistical distribution of galaxies, and various theoretical models based on physical or mathematical arguments have been proposed to fit the observational data (Fry 1986). Although, in principle, this measure contains mathematically complete information on the statistics, it is difficult to relate the count analysis to the visual image or connectivity of galaxy clustering, such as filamentary networks, sheetlike or bubblelike structures, etc.

As a statistical measure to characterize such a topological structure of a galaxy distribution, the genus number has been widely used in the analysis of recent redshift surveys (Gott, Melott, & Dickinson 1986; Gott, Weinberg, & Melott 1987; Weinberg, Gott, & Melott 1987; Melott, Weinberg, & Gott 1988; Gott et al. 1989; Park & Gott 1991; Park, Gott, & da Costa 1992; Weinberg & Cole 1992; Moore et al. 1992; Vogeley et al. 1994; Rhoads, Gott, & Postman 1994). However, the value of the genus had been calculated theoretically only for the random Gaussian field (Adler 1981; Doroshkevich 1970; Bardeen et al. 1986; Hamilton, Gott, & Weinberg 1986), except for some restricted cases, such as for Rayleigh-Lévy random-walk fractals (Hamilton 1988) or unions of overlapping balls (Okun 1990). Hence, at best, what one could have done was to estimate the genus number on large scales that are still in the linear regime, to test the validity of random Gaussian initial conditions.

The situation was somewhat improved recently because a lowest order correction to the Gaussian genus number was analytically obtained by one of us, using the multidimensional Edgeworth expansion around the Gaussian distribution (Matsubara 1994). A detailed comparison has also been made with the results of *N*-body simulations, and it has been shown that the new formula fits the numerical data well in the semilinear regime but not in the nonlinear regime (Matsubara & Suto 1996). This is in accord with the fact that the one-point probability distribution function (PDF) based on the Edgeworth series ceases to fit the count-in-cells once the root mean square (rms) value of the density contrast becomes as large as $\simeq \frac{1}{4}$ (Juszkiewicz et al. 1995; Ueda & Yokoyama 1995). Thus, it is also desirable to find an analytic expression of the genus number for realistic non-Gaussian distributions, just as various non-Gaussian models have been proposed for count-in-cells statistics (Fry 1986).

In the present paper, we present analytic formulae of the genus number for some non-Gaussian distributions in which the density contrast is given by a nontrivial function of either a single Gaussian-distributed random number or its combinations (such non-Gaussian distributions were applied to two-dimensional peak statistics by Coles & Barrow 1987). The former includes the lognormal distribution, which has been used as a model of galaxy distribution ever since Hubble (1934). The lognormal model is found to fit the three-dimensional PDF of observed galaxies (Hamilton 1985; Bouchet et al. 1993; Kofman et al. 1994) and of cell counts in cold dark matter type (CDM-type) *N*-body simulations (Kofman et al. 1994; Ueda & Yokoyama 1995). Coles & Jones (1991) argued for the lognormal mapping of the linear density field to describe its nonlinear evolution in the universe. The latter includes a χ^2 distribution that is closely related to the negative binomial distribution, another widely used distribution with a hierarchical property of higher order cumulants (Fry 1986; Carruthers 1991;

¹ Address after 1995 September 20: Yukawa Institute for Theoretical Physics, Kyoto University, Kyoto 606-01, Japan.

Gaztañaga & Yokoyama 1993; Bouchet et al. 1993). We then compare the new formulae with N -body simulation data having various initial spectra, as well as with the previously known formulae for the Gaussian distribution and second-order perturbation theory.

The rest of the paper is organized as follows. In § 2 we review the derivation of the genus number in a Gaussian distribution and its lowest order correction arising from the three-point correlation function. In § 3 the genus number is given in the case when the density contrast is given by a nontrivial but monotonic function of a Gaussian-distributed quantity. Then in § 4 it is extended to the case in which the density fluctuation is a function of several independent Gaussian variables. In § 5 various analytic formulae of the genus and the PDF are compared with numerical results obtained from N -body simulations. Finally, § 6 is devoted to discussion and conclusions.

2. GENUS CURVE IN A GAUSSIAN DISTRIBUTION AND ITS NONLINEAR CORRECTION THROUGH THE EDGEWORTH SERIES

The genus curve $G(v)$ is defined by $-\frac{1}{2}$ times the total Euler number per unit volume of isodensity contours of a continuous density field. It corresponds to (number of holes – number of isolated regions)/volume. Here the density threshold of the contour is specified by $v \equiv \delta / \langle \delta^2 \rangle^{1/2}$, with δ being the density contrast, which is smoothed appropriately. Mathematically, it is given by the following expectation value:

$$G(v) = -\frac{1}{2} \langle \delta_{\mathbf{D}}(\delta(\mathbf{x}) - v\sigma) \delta_{\mathbf{D}}(\eta_1) \delta_{\mathbf{D}}(\eta_2) | \eta_3 | (\zeta_{11} \zeta_{22} - \zeta_{12}^2) \rangle \quad (1)$$

(Doroshkevich 1970; Adler 1981; Bardeen et al. 1986), where $\eta_i \equiv \partial_i \delta(\mathbf{x}) \equiv \delta_{,i}(\mathbf{x})$, $\zeta_{ij} \equiv \partial_i \partial_j \delta(\mathbf{x}) \equiv \delta_{,ij}(\mathbf{x})$, and $\delta_{\mathbf{D}}$ is Dirac's delta function. Thus, it can in principle be calculated once a seven-point probability distribution function of $\delta(\mathbf{x})$ is known.

In the case when $\delta(\mathbf{x})$ obeys a Gaussian distribution, we find $\delta(\mathbf{x})$, $\eta_i(\mathbf{x})$, and $\zeta_{jk}(\mathbf{x})$ are also Gaussian-distributed, with a vanishing mean and two-body correlations given by

$$\begin{aligned} \langle \delta^2(\mathbf{x}) \rangle &\equiv \sigma^2, & \langle \delta(\mathbf{x}) \eta_i(\mathbf{x}) \rangle &= 0, & \langle \delta(\mathbf{x}) \zeta_{ij}(\mathbf{x}) \rangle &= -\frac{\sigma_1^2}{3} \delta_{ij} \\ \langle \eta_i(\mathbf{x}) \eta_j(\mathbf{x}) \rangle &= \frac{\sigma_1^2}{3} \delta_{ij}, & \langle \eta_i(\mathbf{x}) \zeta_{jk}(\mathbf{x}) \rangle &= 0, & \langle \zeta_{ij}(\mathbf{x}) \zeta_{kl}(\mathbf{x}) \rangle &= \frac{\sigma_2^2}{15} (\delta_{ij} \delta_{kl} + \delta_{ik} \delta_{jl} + \delta_{il} \delta_{jk}), \end{aligned} \quad (2)$$

where σ^2 , σ_1^2 , and σ_2^2 are respectively defined by

$$\sigma^2 \equiv \langle \delta^2 \rangle, \quad \sigma_1^2 \equiv \langle (\nabla \delta)^2 \rangle, \quad \text{and} \quad \sigma_2^2 \equiv \langle (\nabla^2 \delta)^2 \rangle. \quad (3)$$

The final result is

$$G(v) = \frac{1}{(2\pi)^2} \left(\frac{\sigma_1^2}{3\sigma^2} \right)^{3/2} e^{-v^2/2(1-v^2)} \equiv G_{\text{RG}}(v). \quad (4)$$

If the initial fluctuation is a Gaussian random field, linear theory predicts that the genus is described by the Gaussian equation (4) and the PDF by

$$P_{\text{RG}}(v) = \frac{e^{-v^2/2}}{\sqrt{2\pi}}. \quad (5)$$

Next, we consider the correction due to the presence of higher order correlation functions, which arises as a result of nonlinear gravitational evolution, in terms of the multidimensional Edgeworth expansion following Matsubara (1994) and Matsubara & Suto (1996). The final result is

$$G_{2\text{nd}}(v) = -\frac{1}{4\pi^2} \left(\frac{\sigma_1^2}{3\sigma^2} \right)^{3/2} e^{-v^2/2} \left\{ H_2(v) + \sigma \left[\frac{S}{6} H_5(v) + \frac{3T}{2} H_3(v) + 3UH_1(v) \right] + (\sigma^2) \right\}. \quad (6)$$

In the above expression, $H_n(v) \equiv (-1)^n e^{v^2/2} (d/dv)^n e^{-v^2/2}$ is the n th order Hermite polynomial, and S , T , and U are defined as

$$S = \frac{1}{\sigma^4} \langle \delta^3 \rangle, \quad T = -\frac{1}{2\sigma_1^2 \sigma^2} \langle \delta^2 \nabla^2 \delta \rangle, \quad U = -\frac{3}{4\sigma_1^4} \langle \nabla \delta \cdot \nabla \delta \nabla^2 \delta \rangle, \quad (7)$$

respectively, which we call generalized skewness. They come from the three-point correlation function that can be evaluated also by second-order perturbation theory (Matsubara 1994). One should note that generalized skewness should be evaluated for smoothed fluctuations that are evolved nonlinearly. Only after taking into account such smoothing effects, can one compare the second-order perturbation theory with observations. If one uses the Gaussian window with the smoothing length R and assumes the Gaussian initial fluctuations, the generalized skewness is explicitly computed as

$$\begin{aligned} S &= \frac{1}{4\pi^4} [(2 + K)L_{220} + 3L_{131} + (1 - K)L_{222}], \\ T &= \frac{1}{60\pi^4} [5(5 + 2K)L_{240} + 3(9 + K)L_{331} + 15L_{151} + 10(2 - K)L_{242} + 3(1 - K)L_{333}], \\ U &= \frac{1}{140\pi^4} [7(3 + 2K)L_{440} + 21L_{351} - 5(3 + 4K)L_{442} - 21L_{353} - 6(1 - K)L_{444}]. \end{aligned} \quad (8)$$

Here $L_{\alpha\beta n}(R)$ stands for the following integral:

$$L_{\alpha\beta n}(R) \equiv \frac{\sigma_1^{4-\alpha-\beta}}{\sigma^{8-\alpha-\beta}} \int_0^\infty dx \int_0^\infty dy \int_{-1}^1 d\mu e^{-R^2(x^2+y^2+\mu xy)} x^\alpha y^\beta P_n(\mu) P(x) P(y) \quad (9)$$

$$= (-1)^n \sqrt{2\pi} \frac{\sigma_1^{4-\alpha-\beta}}{R \sigma^{8-\alpha-\beta}} \int_0^\infty dx \int_0^\infty dy e^{-R^2(x^2+y^2)} x^{\alpha-1/2} y^{\beta-1/2} I_{n+1/2}(xyR^2) P(x) P(y), \quad (10)$$

where σ and σ_1 are defined by equation (3), in which δ is the Gaussian smoothed density fluctuation of linear theory over the scale R , P_n is the n th order Legendre polynomial, and I_ν is a modified Bessel function. Equations (8)–(10) hold for arbitrary values of the density parameter Ω and cosmological constant Λ . The effect of these parameters manifests itself only through the function $K = K(\Omega, \lambda)$, which depends very weakly on Ω and λ (Bouchet et al. 1992; Bernardeau 1994), where $\lambda \equiv \Lambda/(3H^2)$, H being the Hubble parameter. The explicit form for K has been derived by Matsubara (1995) as

$$K(\Omega, \lambda) = \frac{\Omega}{4} - \frac{\lambda}{2} - \left(\int_0^1 dx X^{-3/2} \right)^{-1} + \frac{3}{2} \left(\int_0^1 dx X^{-3/2} \right)^{-2} \int_0^1 dx X^{-5/2}, \quad (11)$$

where

$$X(x) \equiv \Omega/x + \lambda x^2 + 1 - \Omega - \lambda. \quad (12)$$

In the two specific models we adopt below, we find $K(1, 0) = 3/7 = 0.4286$ and $K(0.2, 0.8) = 0.4335$.

For the power-law fluctuation spectra $P(k) \propto k^n$, the generalized skewness S , T , and U can be written down explicitly in terms of the hypergeometric function as

$$\begin{aligned} S &= 3F\left(\frac{n+3}{2}, \frac{n+3}{2}, \frac{3}{2}; \frac{1}{4}\right) - (n+2 - 2K)F\left(\frac{n+3}{2}, \frac{n+3}{2}, \frac{5}{2}; \frac{1}{4}\right), \\ T &= 3F\left(\frac{n+3}{2}, \frac{n+5}{2}, \frac{3}{2}; \frac{1}{4}\right) - (n+3 - K)F\left(\frac{n+3}{2}, \frac{n+5}{2}, \frac{5}{2}; \frac{1}{4}\right) + \frac{(n-2)(1-K)}{15} F\left(\frac{n+3}{2}, \frac{n+5}{2}, \frac{7}{2}; \frac{1}{4}\right), \\ U &= F\left(\frac{n+5}{2}, \frac{n+5}{2}, \frac{5}{2}; \frac{1}{4}\right) - \frac{n+4-4K}{5} F\left(\frac{n+5}{2}, \frac{n+5}{2}, \frac{7}{2}; \frac{1}{4}\right). \end{aligned} \quad (13)$$

The expressions for S in equations (8) and (13) are derived by Łokas et al. (1995) and are equivalent to the other form independently derived by Matsubara (1994). Similarly, using the function $L_{\alpha\beta n}(R)$, we transform the expressions for T and U presented in Matsubara (1994; eqs. [16] and [18]) which are given here in equations (8) and (13).

The result of equation (6) is the analog of the second-order Edgeworth series of the PDF

$$P_{2nd}(v) = \frac{e^{-v^2/2}}{\sqrt{2\pi}} \left[1 + \sigma \frac{S}{6} H_3(v) + \mathcal{O}(\sigma^2) \right] \quad (14)$$

(Juszkiewicz et al. 1995; Bernardeau & Kofman 1995).

3. THE CASE WHEN THE DENSITY FIELD IS A MONOTONIC FUNCTION OF A RANDOM GAUSSIAN VARIABLE

Next, we turn to evaluation of $G(v)$ for a non-Gaussian distribution whose statistical properties are characterized by a monotonic function F as

$$\delta(\mathbf{x}) = F[\phi(\mathbf{x})], \quad (15)$$

with $\phi(\mathbf{x})$ being a Gaussian-distributed random field with vanishing mean and unit variance, so that one-point PDF of δ reads

$$P(\delta)d\delta = \frac{1}{\sqrt{2\pi} |F'[F^{-1}(\delta)]|} \exp \left\{ -\frac{1}{2} [F^{-1}(\delta)]^2 \right\} d\delta. \quad (16)$$

In this case, we find

$$\eta_i(\mathbf{x}) = F'[\phi(\mathbf{x})] \phi_{,i}(\mathbf{x}), \quad \zeta_{ij}(\mathbf{x}) = F''[\phi(\mathbf{x})] \phi_{,i}(\mathbf{x}) \phi_{,j}(\mathbf{x}) + F'[\phi(\mathbf{x})] \phi_{,ij}(\mathbf{x}). \quad (17)$$

Therefore, $G(v)$ is calculated as

$$\begin{aligned} G(v) &= -\frac{1}{2} \langle \delta_{\mathbf{D}}[F(\phi) - v\sigma] \delta_{\mathbf{D}}[F'(\phi)\phi_{,1}] \delta_{\mathbf{D}}[F'(\phi)\phi_{,2} | F'(\phi)\phi_{,3}] \\ &\quad \times \{ [F''(\phi)\phi_{,1}^2 + F'(\phi)\phi_{,11}] [F''(\phi)\phi_{,2}^2 + F'(\phi)\phi_{,22}] - [F''(\phi)\phi_{,1}\phi_{,2} + F'(\phi)\phi_{,12}]^2 \} \rangle_{\phi} \\ &= -\frac{1}{2} \left\langle \frac{1}{|F'(\phi)|} \delta_{\mathbf{D}}[\phi - F^{-1}(v\sigma)] \frac{\delta_{\mathbf{D}}(\phi_{,1})}{|F'(\phi)|} \frac{\delta_{\mathbf{D}}(\phi_{,2})}{|F'(\phi)|} |F'(\phi)| |\phi_{,3}| F'(\phi)^2 (\phi_{,11}\phi_{,22} - \phi_{,12}^2) \right\rangle_{\phi} \\ &= \frac{1}{(2\pi)^2} \left[\frac{\langle (\nabla\phi)^2 \rangle_{\phi}}{3} \right]^{3/2} \exp \left\{ -\frac{[F^{-1}(v\sigma)]^2}{2} \right\} \{ 1 - [F^{-1}(v\sigma)]^2 \}, \end{aligned} \quad (18)$$

where we have made use of the assumption that $F(\phi)$ is monotonic with nonvanishing $F'(\phi)$.

Thus, the shape of the genus curve is obtained from that of the Gaussian distribution simply by replacing v by $F^{-1}(v\sigma)$. This is as expected, because mapping in terms of a monotonic function does not change the shape of the density profile. Using the relations $\sigma^2 = \langle F(\phi)^2 \rangle_\phi$ and $\sigma_2^2 = \langle F'(\phi)^2 \rangle_\phi \langle (\nabla\phi)^2 \rangle_\phi$ for isotropic spaces, the overall factor can be rewritten to yield the final result:

$$G(v) = \left[\frac{\langle F(\phi)^2 \rangle_\phi}{\langle F'(\phi)^2 \rangle_\phi} \right]^{3/2} G_{\text{RG}}[F^{-1}(v\sigma)]. \tag{19}$$

In the particular case of the lognormal distribution, the function F is defined by

$$F[\phi(x)] = \frac{1}{\sqrt{1 + \sigma^2}} \exp[\sqrt{\ln(1 + \sigma^2)}\phi(x)] - 1. \tag{20}$$

We therefore find the PDF in the lognormal distribution as

$$P_{\text{LN}}(v) = \frac{\sigma}{(1 + v\sigma)\sqrt{2\pi \ln(1 + \sigma^2)}} \exp\left[-\frac{\{\ln[(1 + v\sigma)\sqrt{1 + \sigma^2}]\}^2}{2 \ln(1 + \sigma^2)}\right], \tag{21}$$

and the genus curve in the lognormal distribution as

$$G_{\text{LN}}(v) = \frac{1}{(2\pi)^2} \frac{\sigma_1^3}{[3(1 + \sigma^2) \ln(1 + \sigma^2)]^{3/2}} \exp\left[-\frac{\{\ln[(1 + v\sigma)\sqrt{1 + \sigma^2}]\}^2}{2 \ln(1 + \sigma^2)}\right] \left[1 - \frac{\{\ln[(1 + v\sigma)\sqrt{1 + \sigma^2}]\}^2}{\ln(1 + \sigma^2)}\right]. \tag{22}$$

One can easily check that the above expression reduces to the Gaussian formula in the limit $\sigma \rightarrow 0$.

4. THE CASE WHEN THE DENSITY FIELD DEPENDS ON MULTIPLE GAUSSIAN FIELDS

4.1. General Considerations

We now extend the above analysis to the case when statistical properties of the density field are characterized by a number of independent Gaussian fields $\alpha^a(x)$ through a function f as

$$\delta(x) = f[\alpha^1(x), \alpha^2(x), \dots, \alpha^n(x)]. \tag{23}$$

Here we assume that α^a fields are mutually independent and all have vanishing mean and unit variance. Then, introducing new variables $\beta_i^a \equiv \alpha_{,i}^a$ and $\gamma_{ij}^a \equiv \alpha_{,ij}^a$, we find

$$\eta_i = \frac{\partial f}{\partial \alpha^a} \alpha_{,i}^a \equiv f_a \beta_i^a, \quad \zeta_{ij} = \frac{\partial^2 f}{\partial \alpha^a \partial \alpha^b} \beta_i^a \beta_j^b + \frac{\partial f}{\partial \alpha_i^a} \alpha_{,ij}^a \equiv f_{ab} \beta_i^a \beta_j^b + f_a \gamma_{ij}^a. \tag{24}$$

Here and below, summation over repeated Latin indices a, b, c, \dots, h is implicitly assumed. Then the genus number is formally written as

$$G(v) = -\frac{1}{2} \langle \delta_{\text{D}}(f - v\sigma) \delta_{\text{D}}(f_e \beta_1^e) \delta_{\text{D}}(f_g \beta_2^g) | f_h \beta_3^h | [(f_{ab} \beta_1^a \beta_1^b + f_a \gamma_{11}^a)(f_{cd} \beta_2^c \beta_2^d + f_c \gamma_{22}^c) - (f_{ab} \beta_1^a \beta_2^b + f_a \gamma_{12}^a)^2] \rangle. \tag{25}$$

Here the two-body correlations are given by

$$\begin{aligned} \langle \alpha^a \alpha^b \rangle &= \delta^{ab}, & \langle \alpha^a \beta_i^b \rangle &= 0, & \langle \alpha^a \gamma_{ij}^b \rangle &= -\frac{\hat{\sigma}_1^2}{3} \delta^{ab} \delta_{ij}, & \langle \beta_i^a \beta_j^b \rangle &= \frac{\hat{\sigma}_1^2}{3} \delta^{ab} \delta_{ij}, & \langle \beta_i^a \gamma_{jk}^b \rangle &= 0, \\ \langle \gamma_{ij}^a \gamma_{kl}^b \rangle &= \frac{\hat{\sigma}_2^2}{15} \delta^{ab} (\delta_{ij} \delta_{kl} + \delta_{ik} \delta_{jl} + \delta_{il} \delta_{jk}), \end{aligned} \tag{26}$$

where $\hat{\sigma}_1$ and $\hat{\sigma}_2$ are defined by

$$\hat{\sigma}_1^2 \equiv \langle (\nabla \alpha^p)^2 \rangle \quad \text{and} \quad \hat{\sigma}_2^2 \equiv \langle (\nabla^2 \alpha^p)^2 \rangle. \tag{27}$$

Introducing new variables $\omega_{ij}^a \equiv \gamma_{ij}^a + \hat{\sigma}_1^2 \delta_{ij} \alpha^a / 3$, we find α^a , β_i^b , and ω_{jk}^c are Gaussian random variables whose correlations are totally decoupled from each other:

$$\langle \alpha^a \omega_{jk}^b \rangle = \langle \beta_i^a \omega_{jk}^b \rangle = 0, \quad \langle \omega_{ij}^a \omega_{kl}^b \rangle = \delta^{ab} \left[\left(\frac{\hat{\sigma}_2^2}{15} - \frac{\hat{\sigma}_1^4}{9} \right) \delta_{ij} \delta_{kl} + \frac{\hat{\sigma}_2^2}{15} (\delta_{ik} \delta_{jl} + \delta_{il} \delta_{jk}) \right]. \tag{28}$$

The above fact greatly simplifies the subsequent averaging procedures, because we can average ω_{ij}^a , β_3^b , β_1^c , and β_2^d in turn independently as follows.

First, in

$$\begin{aligned} G(v) &= -\frac{1}{2} \left\langle \delta_{\text{D}}(f - v\sigma) \delta_{\text{D}}(f_e \beta_1^e) \delta_{\text{D}}(f_g \beta_2^g) | f_h \beta_3^h | \right. \\ &\quad \left. \times \left\{ f_a \left(\omega_{11}^a - \frac{\hat{\sigma}_1^2}{3} \alpha^a \right) + f_{ab} \beta_1^a \beta_1^b \right\} \left[f_c \left(\omega_{22}^c - \frac{\hat{\sigma}_1^2}{3} \alpha^c \right) + f_{cd} \beta_2^c \beta_2^d \right] - (f_a \omega_{12}^a + f_{ab} \beta_1^a \beta_2^b)^2 \right\rangle, \end{aligned} \tag{29}$$

averaging over ω_{ij}^a can be readily done using equation (28). The expression in braces should be replaced by

$$\langle \{ \dots \} \rangle_\omega = -\frac{\hat{\sigma}_1^4}{9} f_a f_b (\delta^{ab} - \alpha^a \alpha^b) - \frac{\hat{\sigma}_1^2}{3} f_{ab} (\beta_1^a \beta_1^b + \beta_2^a \beta_2^b) f_c \alpha^c + f_{ab} f_{cd} (\beta_1^a \beta_1^b \beta_2^c \beta_2^d - \beta_1^a \beta_2^b \beta_1^c \beta_2^d). \quad (30)$$

Next, the average over β_3^a is performed, noting that the linear combination $f_h \beta_3^h$ also has a Gaussian distribution with a vanishing mean and the variance

$$\langle (f_h \beta_3^h)^2 \rangle_{\beta_3} = \frac{\hat{\sigma}_1^2}{3} \tilde{f}^2, \quad \text{with} \quad \tilde{f}^2 \equiv \delta^{ab} f_a f_b, \quad (31)$$

to yield

$$\langle |f_h \beta_3^h| \rangle_{\beta_3} = \sqrt{\frac{2}{3\pi}} \tilde{f} \hat{\sigma}_1. \quad (32)$$

We assume that only the nonvanishing \tilde{f} contributes to the final result. The averaging over β_1^a or β_2^a is more involved, but it can be done utilizing the fact that $u_i \equiv f_a \beta_i^a$, β_i^p , and β_i^q ($p \neq q$) constitute a trivariate Gaussian distribution with the correlation matrix

$$M = \frac{\hat{\sigma}_1^2}{3} \begin{pmatrix} \tilde{f}^2 & f_p & f_q \\ f_p & 1 & 0 \\ f_q & 0 & 1 \end{pmatrix}. \quad (33)$$

After some straightforward calculations, we find

$$\langle \delta_D(u_i) \rangle_{\beta_i} = \sqrt{\frac{3}{2\pi}} \frac{1}{\tilde{f} \hat{\sigma}_1}, \quad (34)$$

$$\langle \delta_D(u_i) \beta_i^p \beta_i^q \rangle_{\beta_i} = \sqrt{\frac{3}{2\pi}} \frac{1}{\tilde{f} \hat{\sigma}_1} \frac{\tilde{f}^2 \delta_{pq} - f_p f_q}{3 \tilde{f}^2} \hat{\sigma}_1^2, \quad (35)$$

including the case with $p = q$. We thus obtain the following expression for $G(v)$, which leaves only the average over α :

$$G(v) = -\frac{\hat{\sigma}_1^3}{(6\pi)^{3/2}} \left\langle \delta_D(f - v\sigma) \frac{1}{\tilde{f}} \left[(f_a \alpha^a)^2 - \tilde{f}^2 - 2 \left(f_{aa} - \frac{f_{ab} f_a f_b}{\tilde{f}^2} \right) f_c \alpha^c + (f_{aa})^2 - f_{ab} f_{ab} - \frac{2}{\tilde{f}^2} (f_{ab} f_a f_b f_{cc} - f_{ac} f_{bc} f_a f_b) \right] \right\rangle_\alpha. \quad (36)$$

This average cannot be calculated until we specify the function $f(\alpha^a)$. We therefore move on to a specific example of the χ^2 distribution in the next subsection.

4.2. The χ^2 Distribution

In a χ^2 matter distribution, the density field, $\rho(\mathbf{x})$, is given by

$$\rho(\mathbf{x}) = \frac{\bar{\rho}}{n} \sum_{p=1}^n [\alpha^p(\mathbf{x})]^2, \quad (37)$$

where $\bar{\rho}$ is the mean density. The density contrast becomes

$$\delta(\mathbf{x}) = \frac{\rho(\mathbf{x}) - \bar{\rho}}{\bar{\rho}} = \frac{1}{n} \sum_{p=1}^n [\alpha^p(\mathbf{x})]^2 - 1. \quad (38)$$

Hence, we find

$$\sigma^2 = \langle \delta(\mathbf{x})^2 \rangle = \frac{2}{n}. \quad (39)$$

Although n is a positive integer by definition, we can perform an analytic continuation to an arbitrary positive number and replace n by $2/\sigma^2$ using equation (39) in what follows.

Thus, in the χ^2 distribution, the function $f(\alpha)$ is given by

$$f(\alpha) = \frac{\sigma^2}{2} \alpha^a \alpha^a - 1 \equiv \frac{\sigma^2}{2} \tilde{\alpha}^2 - 1, \quad (40)$$

with $f_a = \sigma^2 \alpha^a$ and $f_{ab} = \sigma^2 \delta^{ab}$. We therefore find from equation (36) that

$$\begin{aligned} G(v) &= -\frac{\hat{\sigma}_1^3}{(6\pi)^{3/2}} \langle \delta_D[f(\tilde{\alpha}) - v\sigma] \frac{1}{\sigma^2 \tilde{\alpha}} (\sigma^4 \tilde{\alpha}^4 + \sigma^4 \tilde{\alpha}^2 - 4\sigma^2 \tilde{\alpha}^2 + 2\sigma^4 - 6\sigma^2 + 4) \rangle_\alpha \\ &= \frac{\hat{\sigma}_1^3}{(3\pi)^{3/2}} \frac{1}{\sqrt{1 + v\sigma}} \left[1 - v^2 - \frac{\sigma(v + \sigma)}{2} \right] P_{CH}(v) \equiv G_{CH}(v). \end{aligned} \quad (41)$$

Here $P_{\text{CH}}(v)$ is the one-point PDF of $\delta(x)/\sigma$ as a function of the threshold v , which is calculated as

$$\begin{aligned} P_{\text{CH}}(v) &\equiv \langle \delta_{\text{D}}(f(\tilde{\alpha})/\sigma - v) \rangle \\ &= \int \frac{d^n \alpha^a}{(2\pi)^{n/2}} e^{-\tilde{\alpha}^2/2} \delta_{\text{D}}\left(\frac{\sigma}{2} \tilde{\alpha}^2 - \frac{1}{\sigma} - v\right) \\ &= \frac{(1 + v\sigma)^{n/2-1}}{\sigma^{n-1} \Gamma(n/2)} \exp\left(-\frac{1 + v\sigma}{\sigma^2}\right) \\ &= \frac{(1 + v\sigma)^{\sigma-2-1}}{\sigma^{2\sigma-2-1} \Gamma(\sigma-2)} \exp\left(-\frac{1 + v\sigma}{\sigma^2}\right). \end{aligned} \quad (42)$$

Using the relation

$$\sigma_1^2 = 3 \langle \eta_1^2 \rangle = 3 \langle f_a \beta_1^a \rangle = \sigma^4 \tilde{\sigma}_1^2 n = 2\sigma^2 \tilde{\sigma}_1^2, \quad (43)$$

we finally obtain

$$G_{\text{CH}}(v) = \frac{1}{(2\pi)^{3/2}} \left(\frac{\sigma_1^2}{3\sigma^2}\right)^{3/2} \left[1 - v^2 - \frac{\sigma(v + \sigma)}{2}\right] \frac{(1 + v\sigma)^{\sigma-2-3/2}}{\Gamma(\sigma-2)\sigma^{2\sigma-2-1}} \exp\left(-\frac{1 + v\sigma}{\sigma^2}\right). \quad (44)$$

Since equation (42) reduces to the Gaussian distribution for $\sigma \rightarrow 0$, equation (44) also coincides with equation (4) in this limit.

Note that equation (42) indicates that the one-point PDF of the density field obeys the negative binomial distribution,

$$P_{\text{NB}}[\rho(x)]d\rho = \frac{1}{\Gamma(\sigma-2)\sigma^2} \left(\frac{\rho}{\bar{\rho}\sigma^2}\right)^{\sigma-2-1} \exp\left(-\frac{\rho}{\bar{\rho}\sigma^2}\right) \frac{d\rho}{\bar{\rho}}. \quad (45)$$

The negative binomial distribution is often used to fit the data of a counts-in-cells analysis, namely, as a model of a PDF of a smoothed density field. A number of observational analyses have shown that it fits the counts-in-cells histogram well for some volume-limited redshift samples (Gaztañaga & Yokoyama 1993; Bouchet et al. 1993). We also note that this distribution has a hierarchical property of higher order connected moments. That is, the N th order cumulant κ_N is given by $\kappa_N = (N-1)!(\kappa_2)^{N-1} = (N-1)!\sigma^{2N-2}$.

On the other hand, in site of the above similarity, the χ^2 distribution and the negative binomial distribution are essentially different from each other once spatial dependence is taken into account. To illustrate it, let us consider two- and three-point correlation functions, ξ and ζ , respectively, in the χ^2 distribution. The former is calculated as

$$\xi(x, y) \equiv \langle \delta(x)\delta(y) \rangle = \frac{\sigma^4}{4} \langle \alpha^a(x)\alpha^a(x)\alpha^b(y)\alpha^b(y) \rangle - 1 = \sigma^2 w^2(x, y), \quad (46)$$

where $\langle \alpha^a(x)\alpha^b(y) \rangle \equiv \delta^{ab} w(x, y)$. Similarly, the latter is given by

$$\begin{aligned} \zeta(x, y, z) &\equiv \langle \delta(x)\delta(y)\delta(z) \rangle \\ &= 2\sigma^4 w(x, y)w(y, z)w(z, x) \\ &= 2\sigma [\xi(x, y)\xi(y, z)\xi(z, x)]^{1/2}, \end{aligned} \quad (47)$$

which is very different from a hierarchical form. On the other hand, if the negative binomial distribution would fit the counts-in-cells analysis for any shape and size of the sampling cell, we would expect the following relation to hold:

$$\zeta(x, y, z) \cong \frac{2}{3} [\xi(y, z)\xi(z, x) + \xi(z, x)\xi(x, y) + \xi(x, y)\xi(y, z)], \quad (48)$$

with the observed slope of the power-law two-point correlation function (Gaztañaga & Yokoyama 1993). Thus, the two distributions should be distinguished from each other even if the one-point PDF has exactly the same form.

5. COMPARISON WITH NUMERICAL SIMULATIONS

We measure the genus of the four data sets from cosmological N -body simulations with random Gaussian initial conditions, kindly provided by T. Suginoara and Y. Suto. Three models are evolved in the Einstein–de Sitter universe with the scale-free initial fluctuation spectra (at expansion factor $a = 1.0$):

$$P(k) \propto k^n \quad (n = -1, 0, \text{ and } 1). \quad (49)$$

The last model corresponds to a spatially flat low-density cold dark matter (LCDM) model. In this specific example, we assume $\Omega_0 = 0.2$, $\lambda_0 = 0.8$, and $h = 1.0$ (Suginoara & Suto 1991). The amplitude of the power spectrum in the LCDM model at $a = 6$ is normalized so that the top-hat smoothed rms mass fluctuation is unity at $8 h^{-1}$ Mpc. In fact, this LCDM model can be regarded as representing a specific example of the most successful cosmological scenarios so far (e.g., Suto 1993). All models are evolved with a hierarchical tree code implementing the fully periodic boundary condition in a cubic volume of L^3 . The physical comoving size of the computational box in the LCDM model is $L = 100 h^{-1}$ Mpc. The number of particles employed in the simulations is $N = 64^3$, and the gravitational softening length is $\epsilon_g = L/1280$ in the comoving frame. Further

details of the simulation models and other extensive analyses are described in Hernquist, Bouchet, & Suto (1991), Suginozaka et al. (1991), Suginozaka & Suto (1991), Suto (1993), Matsubara & Suto (1994), and Suto & Matsubara (1994).

The computation of the genus from the particle data is performed using the code kindly provided by D. Weinberg (Weinberg 1988; Gott et al. 1989). In short, the procedure goes as follows: (1) The computational box is divided into N_c^3 ($=128^3$) cubes, and the density $\rho_g(\mathbf{r})$ at the center of each cell is computed using a cloud-in-cell density assignment. (2) The Fourier transform

$$\tilde{\rho}_g(\mathbf{k}) \equiv \frac{1}{L^3} \int \rho_g(\mathbf{r}) \exp(i\mathbf{k} \cdot \mathbf{r}) d^3r \quad (50)$$

is convolved with the Gaussian filter and transformed back to define a *smoothed* density of each cell (with the filtering length R_f):

$$\rho_s(\mathbf{r}; R_f) = \frac{L^3}{8\pi^3} \int \tilde{\rho}_g(\mathbf{k}) \exp\left(-\frac{k^2 R_f^2}{2} - i\mathbf{k} \cdot \mathbf{r}\right) d^3k. \quad (51)$$

(3) The rms amplitude of the density fluctuations is computed directly from the smoothed density:

$$\sigma(R_f) \equiv \sqrt{\langle (\rho_s/\bar{\rho} - 1)^2 \rangle}, \quad (52)$$

where $\bar{\rho}$ is the mean density of the particles. (4) The isodensity surface of the critical density

$$\rho_c \equiv [1 + \nu\sigma(R_f)]\bar{\rho} \quad (53)$$

is approximated by the boundary surface of the high-density ($\rho_s > \rho_c$) and low-density ($\rho_s < \rho_c$) cells. (5) Then the genus of the surface is computed by summing up the angle deficit $D(i, j, k)$ at the vertex of cell (i, j, k) :

$$g_s(\nu) = -\frac{1}{4} \sum_{i,j,k=1}^{N_c} D(i, j, k). \quad (54)$$

The way to compute $D(i, j, k)$ is detailed in Gott et al. (1986). The genus curve $G(\nu)$ is defined to be the number of genera per unit volume as a function of the threshold ν . (6) We repeated the above procedure 50 times using the bootstrap resampling method (Ling, Frenk, & Barrow 1986) in order to estimate the statistical errors of $G(\nu)$.

It should be noted that earlier papers (e.g., Gott et al. 1989; Rhoads et al. 1994; Vogeley et al. 1994) *defined* the density threshold ν of genus curves so that the volume fraction on the high-density region of the isodensity surface is equal to

$$f = \frac{1}{\sqrt{2\pi}} \int_{\nu}^{\infty} e^{-t^2/2} dt. \quad (55)$$

Adopting this method, the lognormal model and random Gaussian model would not be distinguished from each other (Coles & Jones 1991). Since we intend to distinguish them in order to see whether or not the lognormal model can fit the genus number, we adopt the straightforward definition $\delta = \nu\sigma$ of the density threshold throughout this paper.

To obtain the normalized genus curve $G(\nu)/G(0)$, we follow the method developed in Matsubara & Suto (1996). In practice, we first compute $G(\nu)$ at 51 bins (in equal intervals) for $-3 \leq \nu \leq 3$. Then, we estimate the amplitude of $G(0)$ by χ^2 -fitting the seven data points around $\nu = 0$ to the lognormal formula of equation (22) so that the computed value of $G(0)$ is less affected by the statistical fluctuation at one data point. The result is almost insensitive to which fitting formula we use in estimating $G(0)$.

The PDFs, $P(\nu)$, which have been similarly computed with 50 bootstrap resampling errors, and normalized genus curves, $G(\nu)/G(0)$, are plotted in Figures 1–3 for power-law models with $n = -1, 0$, and 1 , respectively. We select three different sets of the expansion factor a ($=1$ at the initial epoch) and the filtering length R_f for each model, so that the resulting $\sigma(R_f)$ covers from weakly to fully nonlinear regimes. The upper panels show the PDF and lower panels show the genus curves. The results of a random Gaussian distribution (eqs. [4] and [5]) are plotted in dotted curves, those of second-order perturbation theory (eqs. [14] and [6] with eq. [13]) in dashed curves, lognormal formulae (eqs. [21] and [22]) in solid curves, and χ^2 formulae (eqs. [42] and [44]) in dot-dashed curves. Symbols indicate the results of N -body simulations. The curves for random Gaussian and second-order perturbation theory using Edgeworth series are not guaranteed a vanishing genus for the negative density. We have forced these theoretical curves to be zero in the relevant regions in the plot.

The comparison of genus curves between the N -body results and the theories based on the Edgeworth series are described in detail in Matsubara & Suto (1996), so we do not repeat the detailed argument here. In short, these two curves agree well for $-0.2 \lesssim \nu\sigma \lesssim 4$, where perturbation theory is expected to be valid, but the extrapolation of the second-order formula beyond this regime does not work.

As for the PDFs, the lognormal model fits the simulation results fairly well from weakly to fully nonlinear regimes. The degree of agreement, however, depends on the initial power spectrum. It works best for $n = 0$ model. Note that we use the Gaussian window. Usually, the lognormal model is applied to the counts-in-cells analysis which corresponds to the top-hat window. For the top-hat window, the $n = -1$ model fits the lognormal model better than the $n = 0$ model (Bernardeau & Kofman 1995). Other non-Gaussian curves, including χ^2 distributions, fit simulation data well in weakly nonlinear regimes, while they deviate considerably from simulation results on fully nonlinear regimes.

For the genus, the lognormal model is also the best among the non-Gaussian distributions considered here. The degree of agreement between the lognormal model and simulation results also depends on the initial power spectrum. The fitting is the

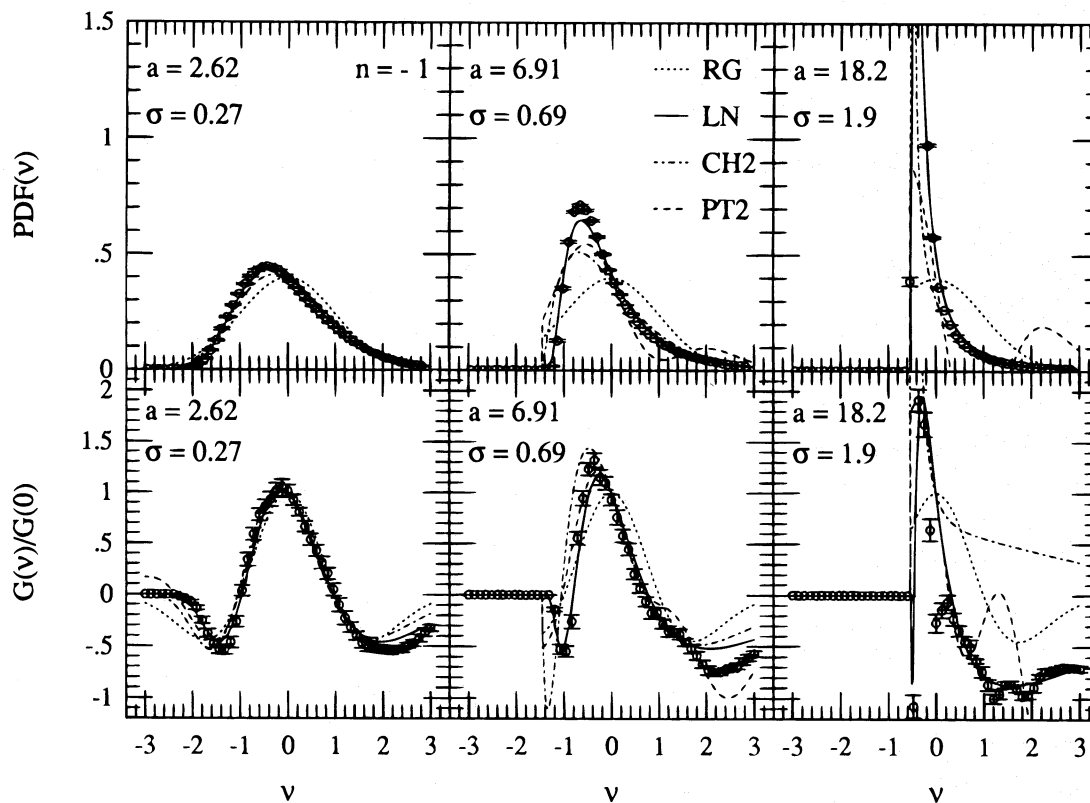


FIG. 1.—PDFs (upper panels) and normalized genus curves (lower panels) from the N -body simulation data for the $n = -1$ power-law model ($\Omega_0 = 1$, $\lambda_0 = 0$) are plotted by open circles. Three different sets of the expansion factor a ($=1$ at the initial epoch) are selected, and the Gaussian window function with the filtering length $R_f = L/25$ is used. The values of the expansion factor and the resulting variance σ are indicated in the figure. The theoretical prediction for the random Gaussian field is plotted by dotted lines, the lognormal model by solid lines, the χ^2 model by dot-dashed lines, and second-order perturbation theory by dashed lines.

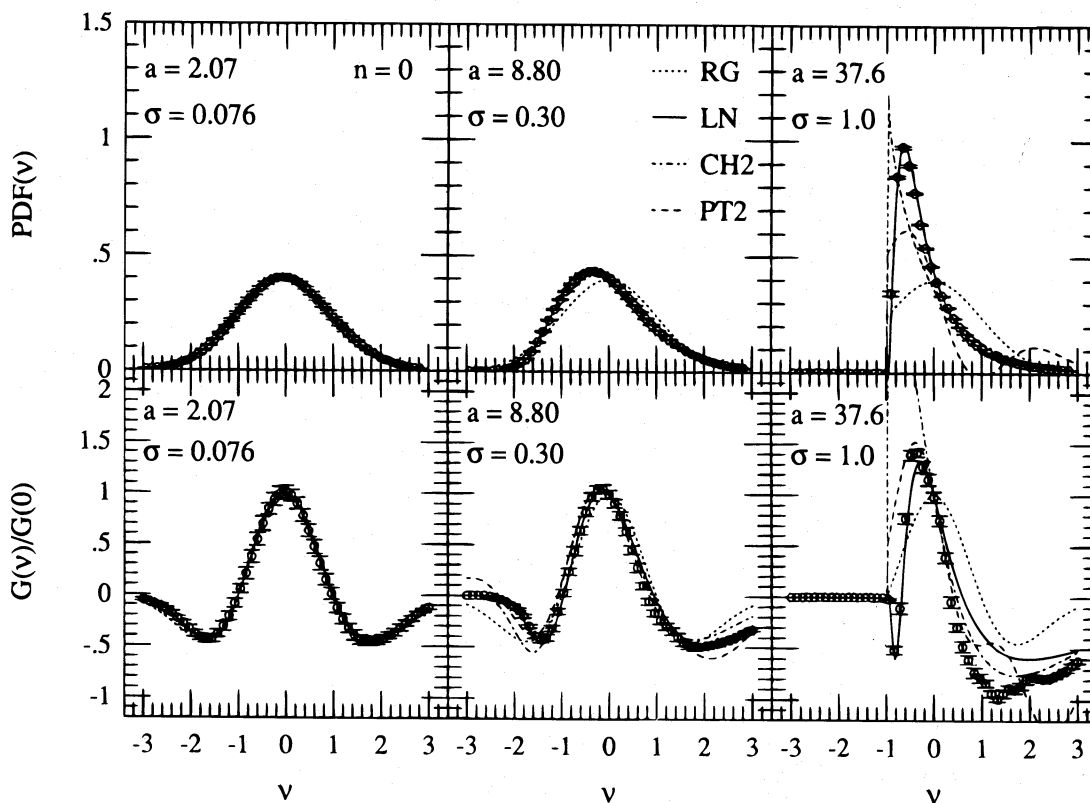


FIG. 2.—Same as Fig. 1, but for the $n = 0$ power-law model

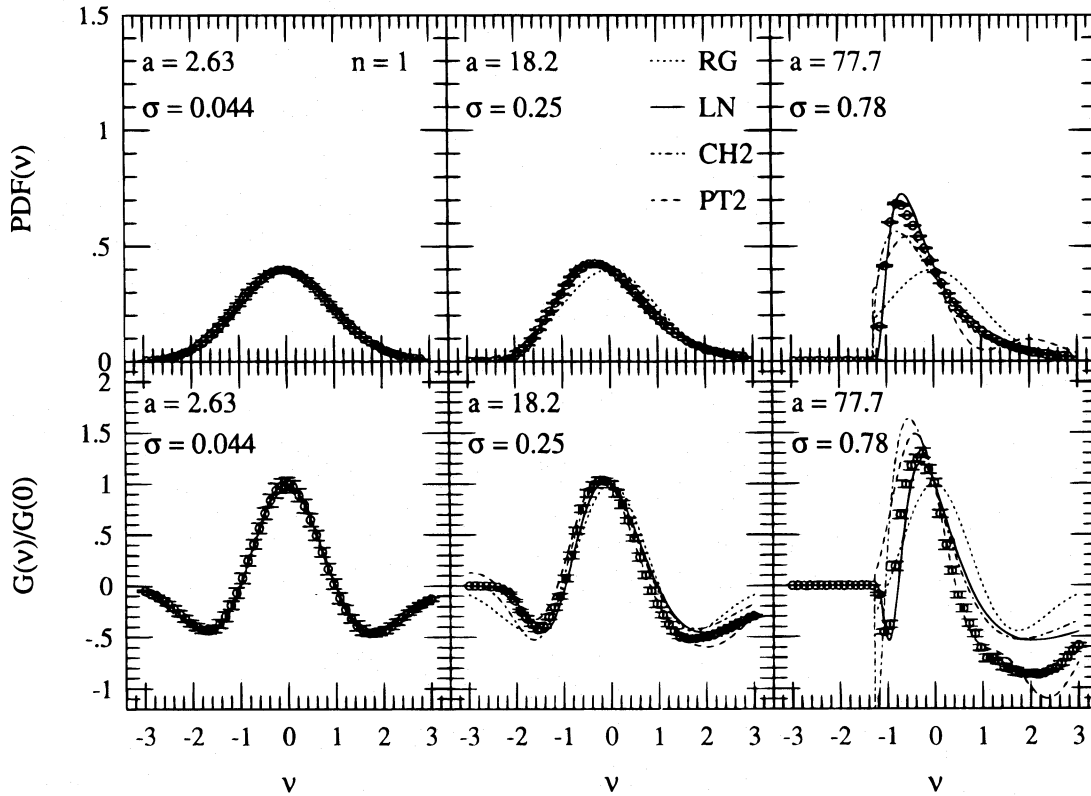


FIG. 3.—Same as Fig. 1, but for the $n = 1$ power-law model

best for the $n = -1$ model. For other models, the lognormal model does not fit well in positive threshold regions ($v > 0$). For all the simulation results, the agreement of the lognormal model happens to be better than weakly nonlinear formula for negative threshold regions. This may be partly due to the fact that the weakly nonlinear formula cannot naturally take into account the positivity of the density, but the lognormal model achieves it by construction. On the other hand, the χ^2 model

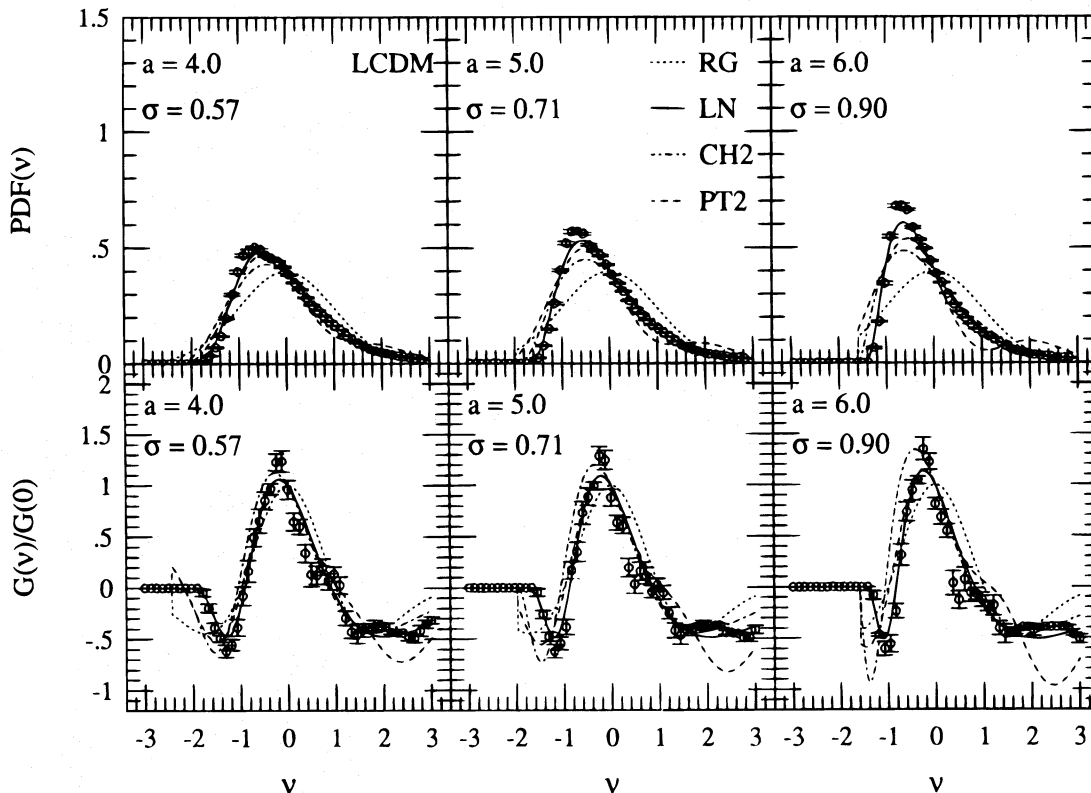


FIG. 4.—Same as Fig. 1, but for the low-density cold dark matter model ($\Omega_0 = 0.2$, $\lambda_0 = 0.8$, $h = 1.0$). The adopted Gaussian filtering length R_f corresponds to $4 h^{-1}$ Mpc (comoving). The top-hat smoothed rms mass fluctuation at $a = 6$ is unity at $8 h^{-1}$ Mpc.

does not agree well with any simulation results except for the initial linear regime, even if it assures the positivity of the density.

In Figure 4 are plotted the PDFs and normalized genus curves for the LCDM model for an example of a realistic cosmological scenario. The smoothing length R is $4 h^{-1}$ Mpc. If galaxies trace mass, $a = 6$ corresponds to the present epoch ($z = 0$). Thus, $a = 4$ and $a = 5$ correspond to $z = 0.5$ and $z = 0.2$, respectively. We find that our simulation results of the LCDM model and the lognormal model for Gaussian smoothed PDFs agree fairly well, except for some differences of the peak height. See also Ueda & Yokoyama (1995) for top-hat smoothed PDFs. For the normalized genus curves, the lognormal model fits the simulation results well.

6. CONCLUSIONS AND DISCUSSION

In the present paper, we have derived theoretical predictions of the genus statistics for some non-Gaussian distributions. We have calculated the expectation value of the genus number for non-Gaussian fields that are given by nontrivial functions of Gaussian random fields. Two specific fields of this category, the lognormal distribution and the χ^2 distribution, were investigated in detail.

As is seen in the figures, the one-point PDF of the smoothed density field is fitted by the lognormal model fairly well for all the simulated models adopted here, i.e., power-law models with $n = -1, 0$, and 1 , and the LCDM model. The lognormal formula for the genus curve also works well to fit all the simulation data in the negative threshold regions. But considerable deviation is observed in the positive threshold regions in the nonlinear regime of the power-law models with $n = 0$ and 1 . On the other hand, the formula fits the entire regions of $n = -1$ and the LCDM models fairly well. Thus the genus statistic is more appropriate than the one-point PDF to distinguish between various initial power spectra for a Gaussian smoothed field. This is due to the fact that the former depends on the spatial derivatives of the density field, too.

Several arguments exist to explain the validity of the lognormal model as a statistical distribution in nonlinear regimes. Coles & Jones (1991) argue that the lognormal distribution is obtained from the continuity equation in the nonlinear regime, but with linear or Gaussian velocity fluctuations, so that it may be adopted as a model to describe statistics in the weakly nonlinear regime. On the other hand, Bernardeau & Kofman (1995) claim its successful fit to the PDF of CDM-type simulations is just a coincidence due to the particular shape of the CDM power spectrum based on the top-hat smoothing. Since the LCDM power spectrum has a similar structure to the $n = -1$ power law on the scales of interest, our genus curve results are consistent with these arguments.

Observationally, the negative binomial distribution, which has the same one-point PDF as the χ^2 distribution, has been shown to fit the counts-in-cells of various redshift samples well (Gaztañaga & Yokoyama 1993; Bouchet et al. 1993). However, our results indicate that the χ^2 formulae reproduce neither the one-point PDF nor the genus curve of the simulations. Does that imply that these N -body simulations have nothing to do with the real universe? Not necessarily, because here we are extracting information on relatively small length scales $R \sim 4 h^{-1}$ Mpc using all the 64^3 particles in the simulations, while the observational counts analysis has been performed on larger scales using volume-limited samples with a much smaller number density of galaxies. The effect of sparse sampling in the counts analysis has been analyzed by Ueda & Yokoyama (1995) for the LCDM model, and it has been shown that the χ^2 or the negative binomial PDF does not fit the data well if we use all the particles in the simulation, but it fits well if we use sparsely sampled data with a similar number density to that of the volume-limited samples currently available.

Thus, our results do not rule out the LCDM model. On the contrary, it remains one of the most promising models of our universe (e.g., Suto 1993). To test the LCDM model further, we can use the genus statistic by examining whether it is fitted by the lognormal formula. Although the presently available redshift data are not statistically significant enough (e.g., Vogeley et al. 1994) to extract a specific conclusion, we can reasonably expect that the statistical significance of the observed genus curve will improve rapidly in the near future.

Now that we have obtained a number of theoretical formulae for the genus curve, we can make use of it not only to test the Gaussianity of the primordial fluctuations but also to discriminate between various models of structure formation.

We are grateful to Yasushi Suto for providing us with his N -body simulation data and helping us to plot the genus curves from simulation data, and to David Weinberg for providing us with the routines to compute the genus curve from numerical data. T. M. gratefully acknowledges the fellowship from the Japan Society of Promotion of Science. This research was supported in part by Grants-in-Aid by the Ministry of Education, Science, and Culture of Japan (No. 0042).

REFERENCES

- Adler, R. J. 1981, *The Geometry of Random Fields* (Chichester: Wiley)
- Bardeen, J. M., Bond, J. R., Kaiser, N., & Szalay, A. S. 1986, *ApJ*, 304, 15
- Bernardeau, F. 1994, *ApJ*, 433, 1
- Bernardeau, F., & Kofman, L. 1995, *ApJ*, 443, 479
- Bouchet, F. R., Juszkiewicz, R., Columbi, S., & Pellat, R. 1992, *ApJ*, 394, L5
- Bouchet, F. R., Strauss, M. A., Davis, M., Fisher, K. B., Yahil, A., & Huchra, J. 1993, *ApJ*, 417, 36
- Carruthers, P. 1991, *ApJ*, 380, 24
- Coles, P., & Barrows, J. D. 1987, *MNRAS*, 228, 407
- Coles, P., & Jones, B. 1991, *MNRAS*, 248, 1
- Doroshkevich, A. G. 1970, *Astrophysics*, 6, 320
- Fry, J. N. 1986, *ApJ*, 306, 358
- Gaztañaga, E., & Yokoyama, J. 1993, *ApJ*, 403, 450
- Gott, J. R., et al. 1989, *ApJ*, 340, 625
- Gott, J. R., Melott, A. L., & Dickinson, M. 1986, *ApJ*, 306, 341
- Gott, J. R., Weinberg, D. H., & Melott, A. L. 1987, *ApJ*, 319, 1
- Hamilton, A. J. S. 1985, *ApJ*, 292, L35
- . *PASP*, 100, 1343
- Hamilton, A. J. S., Gott, J. R., & Weinberg, D. 1986, *ApJ*, 309, 1
- Hernquist, L., Bouchet, F. R., & Suto, Y. 1991, *ApJS*, 75, 231
- Hubble, E. 1934, *ApJ*, 79, 8
- Juszkiewicz, R., Weinberg, D. H., Amsterdamski, P., Chodorowski, M., & Bouchet, F. 1995, *ApJ*, 442, 39
- Kofman, L. A., Bertschinger, E., Gelb, M. J., Nusser, A., & Dekel, A. 1994, *ApJ*, 420, 44
- Ling, E. N., Frenk, C. S., & Barrow, J. D. 1986, *MNRAS*, 223, 21P
- Lokas, E. L., Juszkiewicz, R., Weinberg, D. H., & Bouchet, F. R. 1995, *MNRAS*, 274, 730
- Matsubara, T. 1994, *ApJ*, 434, L43
- . 1995, *Prog. Theor. Phys. Lett.*, 94, 1151
- Matsubara, T., & Suto, Y. 1994, *ApJ*, 420, 497
- . 1996, *ApJ*, 460, 51

- Melott, A. L., Weinberg, D. H., & Gott, J. R. 1988, ApJ, 328, 50
Moore, B., et al. 1992, MNRAS, 256, 477
Okun, B. L. 1990, J. Stat. Phys., 59, 523
Park, C., & Gott, J. R. 1991, ApJ, 378, 457
Park, C., Gott, J. R., & da Costa, L. N. 1992, ApJ, 392, L51
Rhoads, J. E., Gott, J. R., & Postman, M. 1994, ApJ, 421, 1
Suginohara, T., & Suto, Y. 1991, PASJ, 43, L17
Suginohara, T., Suto, Y., Bouchet, F. R., & Hernquist, L. 1991, ApJS, 75, 631
Suto, Y. 1993, Prog. Theor. Phys., 90, 1173
Suto, Y., & Matsubara, T. 1994, ApJ, 420, 504
Totsuji, H., & Kihara, T. 1969, PASJ, 21, 221
Ueda, H., & Yokoyama, J. 1995, YITP/U-94-27 preprint, astro-ph/9501041
Vogeley, M. S., Park, C., Geller, M. J., Huchra, J. P., & Gott, J. R. 1994, ApJ, 420, 525
Weinberg, D. H. 1988, PASP, 100, 1373
Weinberg, D. H., & Cole, S. 1992, MNRAS, 259, 652
Weinberg, D. H., Gott, J. R., & Melott, A. L. 1987, ApJ, 321, 2
White, S. D. M. 1979, MNRAS, 186, 145